JOURNAL OF AIRCRAFT
Vol. 46, No. 4, July–August 2009

Engineering Notes

Stability and Flying Qualities of an Unmanned Airplane Using the Vortex-Lattice Method

Elsa M. Cárdenas,* Pedro J. Boschetti,† and Andrea Amerio‡
Universidad Simón Bolívar, 1080 Caracas, Venezuela

DOI: 10.2514/1.44306

Nomenclature

C_{Lq}, C_{Mq}	=	variation of lift and pitching moment coefficients with pitch rate
$C_{L\alpha}$, $C_{D\alpha}$, $C_{M\alpha}$	=	lift, drag, and pitching moment slopes
$C_{L\dot{\alpha}}$, $C_{M\dot{\alpha}}$	=	variation of lift and pitching moment coefficients with rate of change of angle of attack
$C_{L\delta}$, $C_{M\delta}$	=	variation of lift and pitching moment coefficients with elevator deflection
$C_{\ell p}$, C_{np}, C_{Yp}	=	variation of rolling, yawing, and side force coefficients with roll rate
$C_{\ell r}$, C_{nr}, C_{Yr}	=	variation of rolling, yawing, and side force coefficients with yaw rate
$C_{\ell\beta}$, $C_{n\beta}$, $C_{Y\beta}$	=	variation of rolling, yawing, and side force coefficients with sideslip angle
$C_{\ell\delta r}$, $C_{n\delta r}$, $C_{Y\delta r}$	=	variation of rolling, yawing, and side force coefficients with rudder angle
$C_{\ell\delta a}$, $C_{n\delta a}$, $C_{Y\delta a}$	=	variation of rolling, yawing, and side force coefficients with aileron angle
c	=	mean aerodynamic chord
p, q, r	=	roll, pitch, and yaw rate
T	=	period
$t_{1/2}$, $N_{1/2}$	=	time and number of cycles to half-amplitude
u, w	=	longitudinal and vertical components of velocity
α	=	angle of attack
β	=	sideslip angle
δ_e, δ_r, δ_a	=	elevator, rudder, and aileron deflection
ζ	=	damping ratio
θ, Φ	=	pitch and bank angle
λ	=	eigenvalue
ω_n	=	undamped natural frequency

I. Introduction

THE Unmanned Aerial Vehicle for Ecological Conservation (ANCE) is a small, twin-boom, pusher-propeller airplane with a maximum takeoff mass of 182.055 kg, capable of carrying 40 kg of payload in the form of a high-technology camera to find oil leakages during daylight or at night [1,2]. The propeller is powered by a 26 kW two-stroke engine with two pistons. The wingspan of the vehicle is 5.187 m, with a rectangular straight wing with local twist [3], no dihedral, a surface area of 3.13 m^2, and a wing aspect ratio of 8.57. The wing section is a NACA 4415 airfoil along the whole wingspan. No high-lift devices were included in the design. It is expected that the ANCE will have a cruise speed of 41.18 m/s at 2438 m above sea level for a wing Reynolds number of 1.413×10^6 [1,2].

The objective of this work is to make a preliminary evaluation of the static stability and open-loop dynamic stability for the unpowered condition by inviscid computational fluid dynamics. The derivative data obtained from the static stability analysis were used to determine the dynamic stability and response characteristics, followed by an analysis to evaluate the airplane's flying qualities.

The static stability was evaluated using a vortex-lattice method code called Tornado [4]. There is no previous experimental data for moments and side force to do a complete validation of the data obtained by the inviscid computational fluid dynamics method. For this reason, the research is a preliminary analysis. However, the vortex-lattice method has been found to be a very useful preliminary design tool [5]. Comparison with the experimental data shows good agreement with the force and moment coefficients due to lift in a subsonic regime [5–8]. Specifically, Tornado has been evaluated to estimate static stability derivates. It was demonstrated that the longitudinal derivates computed with Tornado are in good agreement with the experimental data and that the lateral-directional derivates calculated are acceptable [9].

II. Vortex-Lattice Method

Tornado, version T131b [4], was used to calculate the forces and moments of the airplane. Tornado is a three-dimensional vortex-lattice open-source program written in MATLAB®. This code models any number of three-dimensional wing surfaces and calculates three-dimensional forces and aerodynamic coefficients.

The vortex-lattice method represents the wing as a planar surface broken into quadrilateral panels on which a horseshoe vortex is superimposed. The law of Biot–Savart is used to calculate the velocities induced by each horseshoe vortex at a specific control point. A set of linear algebraic equations for the horseshoe-vortex strengths is obtained when all control points on the wing are summed, satisfying the boundary condition of no flow through the wing. The wing circulation and the pressure differential between the upper and lower surfaces are connected to the vortex strengths. Finally, the forces are obtained by integration of the pressure differentials [10,11]. In Tornado, the horseshoe-vortex arrangement of other vortex-lattice codes is replaced with a vortex-sling arrangement. This works in the same way, but the legs of the shoe are flexible and consist of seven vortex elements (instead of three) of equal strength [12].

Figure 1 shows the vortex-lattice grid geometry for the ANCE. The landing gear and the camera are not included in the paneled geometry formed by 1100 panels, because the contribution of these components to the potential flow is assumed to be negligible. The fuselage and booms were idealized with cruciform shapes [13]; this body simulation is highly computationally efficient for load distribution [6]. This vortex-lattice representation was previously used to model the ANCE without wing twist [3], and the lift and drag coefficients were in good agreement with the experimental data present in [14].

Presented as Paper 306 at the 47th AIAA Aerospace Sciences Meeting, Orlando, FL, 5–8 January 2009; received 11 March 2009; revision received 11 March 2009; accepted for publication 13 March 2009.

*Assistant Professor, Department of Industrial Technology, Sede del Litoral, Valle de Sartenejas, 89000. Member AIAA.
†Assistant Professor, Department of Industrial Technology, Sede del Litoral, Valle de Sartenejas, 89000. Member AIAA.
‡Aggregate Professor, Department of Industrial Technology, Sede del Litoral, Valle de Sartenejas, 89000. Member AIAA.

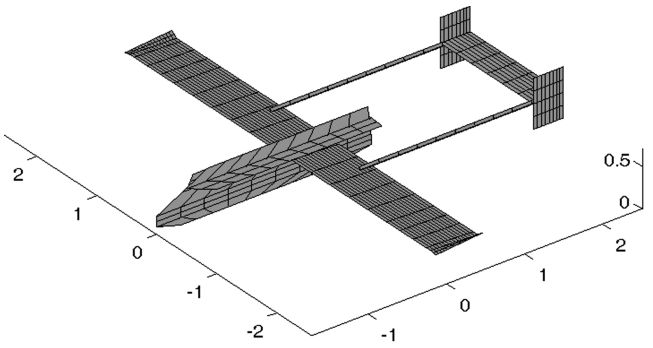

Fig. 1 Vortex-lattice representation of the airplane.

III. Results and Discussion

A. Longitudinal Aerodynamics

The longitudinal aerodynamics was investigated using the angle of attack, the elevator deflection angle, and the pitching rate as variables. The lift coefficient at $\alpha = 0$ deg and $\delta_e = 0$ deg is equal to 0.5116, and it becomes 0.6211 when $\delta_e = 10$ deg. The resultant lift slope is 5.460 rad^{-1}; the variation of the lift coefficient with elevator angle is 0.6818 rad^{-1}. Longitudinal stability was investigated from pitching moment coefficient curves obtained for various elevator angles. The slope of the pitching moment coefficient is -2.727 rad^{-1}, indicating a stable airplane. The moment coefficient at a 0 deg angle of attack is 0.0147, and the pitching moment coefficient with elevator angle is -2.865 rad^{-1}. For the baseline center of gravity at $0.25c$, the neutral point is located at $0.749c$. The slope of the pitching moment coefficient curve with pitch rate is -45.156 s/rad, and the variation of lift coefficient with pitch rate is 18.431 s/rad.

B. Lateral-Directional Aerodynamics

The lateral-directional aerodynamic coefficients were analyzed as a function of the sideslip angle, the rudder and aileron deflections, and the yaw and roll rates at $\alpha = 0$. The side force coefficient due to sideslip has a derivative, $C_{Y\beta} = -0.556$/rad. The airplane is laterally stable with a negative slope of -0.017 rad^{-1}. The directional stability has a positive slope of 0.155 rad^{-1}, meaning that the aircraft is directionally stable.

The side force variation with rudder angle has a derivative, $C_{Y\delta r} = -0.269$/rad; the yawing and roll moment coefficients due to the deflection of the rudder were determined and their derivatives are $C_{n\delta r} = 0.149$/rad and $C_{\ell\delta r} = -0.006$/rad at the zero sideslip condition.

The variation of the rolling coefficient with aileron angle is -0.206 rad^{-1}. It was observed that increasing the aileron angle increases the roll moment. The yawing moment variation with aileron angle has a derivative, $C_{n\delta a} = 0.017$/rad, and the side force variation with aileron angle is -0.001 rad^{-1}.

The side force and the rolling and yawing moments have been studied as a function of the roll and yaw rates. The value of the roll moment coefficient derivatives due to roll rate is -0.751 s/rad; the yawing moment variation with roll rate has a derivative, -0.032 s/rad, and the side force curve slope is 0.075 s/rad. The derivatives of the side force and yawing moment due to yaw rate are -0.644 s/rad and -0.429 s/rad, respectively. Table 1 has a summary of stability derivatives from ANCE calculated by the vortex-lattice method and those estimated from empirical Digital DATCOM [15,16].

C. Longitudinal Motion and Response

The static stability data obtained by the vortex-lattice method were used to determine the airplane dynamic stability response characteristic. The minimum drag coefficient was estimated by the classic technique in [17,18], using the procedure in [3,19]. The rolling, pitching, and yawing moments of inertia used in the analysis are 150, 400, and 400 kg $\cdot$ m^2, respectively. These values were estimated considering the preliminary mass distribution of the ANCE in [20].

The airplane equation of motion is formulated in state space as $x' = Ax + \eta B$, where $x = [\Delta u; \quad \Delta w; \quad \Delta q; \quad \Delta\theta]^T$ is the state vector, $\eta = [\Delta\delta_e]^T$ is the control vector, and the matrices A and B contain the dimensional stability and control derivatives calculated using the corresponding values in Table 1. The matrix A, as defined by Nelson [21], has the following values for the longitudinal dynamics of the airplane:

$$A_{\text{long}} = \begin{bmatrix} -0.01837 & 0.097289 & 0 & -9.81 \\ -0.33199 & 1.768831 & 41.18 & 0 \\ 0.002168 & -0.230063 & -2.26909 & 0 \\ 0 & 0 & 1 & 0 \end{bmatrix}$$

The eigenvalues obtained from this matrix describe the two response longitudinal modes of motion: 1) the short-period mode, $\lambda_{1,2} = -2.0245 \pm 3.067i$; and 2) the phugoid mode, $\lambda_{3,4} = -0.0036 \pm 0.2413i$.

The eigenvalues are complex and have negative real parts. This means that the airplane is dynamically stable. If it receives an initial disturbance, the response would decay sinusoidally in time.

The eigenvalues obtained were used to determine the characteristics of the short-period and phugoid modes. Table 2 contains the calculated values for these characteristics.

The flying qualities of an airplane are related to the dynamic stability characteristics. These are defined with reference to the Cooper and Harper rating scale [22]. The specification of these requirements for airplane flying qualities can be found in [23,24] and for conventional remotely piloted vehicles in [25]. The ANCE is classified according to size and maneuverability as class III in flight phases B and C based on [25]. For short-period motion, these ratings are expressed graphically as a function of damping ratio, control anticipation parameter, undamped natural frequency, and acceleration sensitivity [23–25].

The short-period mode of the ANCE has an acceleration sensitivity of 7.425, a damping ratio equal to 0.55089, an undamped natural frequency of 3.675 rad/s, and a control anticipation parameter equal to 1.8188. It satisfies the requirement for level 1 (category B) for cruise flight phase and level 2 for terminal flight phase (category C). The airplane has a damping ratio at the phugoid

Table 1 Stability derivatives from ANCE given in 1/rad

$C_{L\alpha}$	5.4603	$C_{\ell\beta}$	−0.0172
C_{Lq}	18.4311	$C_{\ell p}$	−0.7512
$C_{L\delta}$	0.6818	$C_{\ell r}$	0.2146
$C_{M\alpha}$	−2.7273	$C_{\ell\delta r}$	−0.0057
C_{Mq}	−45.1563	$C_{\ell\delta a}$	−0.2063
$C_{M\delta}$	−2.8648	$C_{n\beta}$	0.1547
$C_{D\alpha}$	0.2093	C_{np}	−0.0322
$C_{Y\beta}$	−0.5558	C_{nr}	−0.4292
C_{Yp}	0.0751	$C_{n\delta r}$	0.1490
C_{Yr}	−0.6439	$C_{n\delta a}$	0.0172
$C_{Y\delta r}$	−0.2693	$C_{L\dot{\alpha}}$[a]	2.3342
$C_{Y\delta a}$	−0.0011	$C_{M\dot{\alpha}}$[a]	−10.0497

[a]Estimated by Digital DATCOM

Table 2 Longitudinal dynamic characteristics

Phugoid mode	$t_{1/2}$, s	191.6667
	T, s	26.0389
	ζ_p	0.01492
	ω_{np}, rad/s	0.24133
	$N_{1/2}$, cycles	7.3608
Short mode	$t_{1/2}$, s	0.34083
	T, s	2.0486
	ζ_{sp}	0.55089
	ω_{nsp}, rad/s	3.67492
	$N_{1/2}$, cycles	0.16636

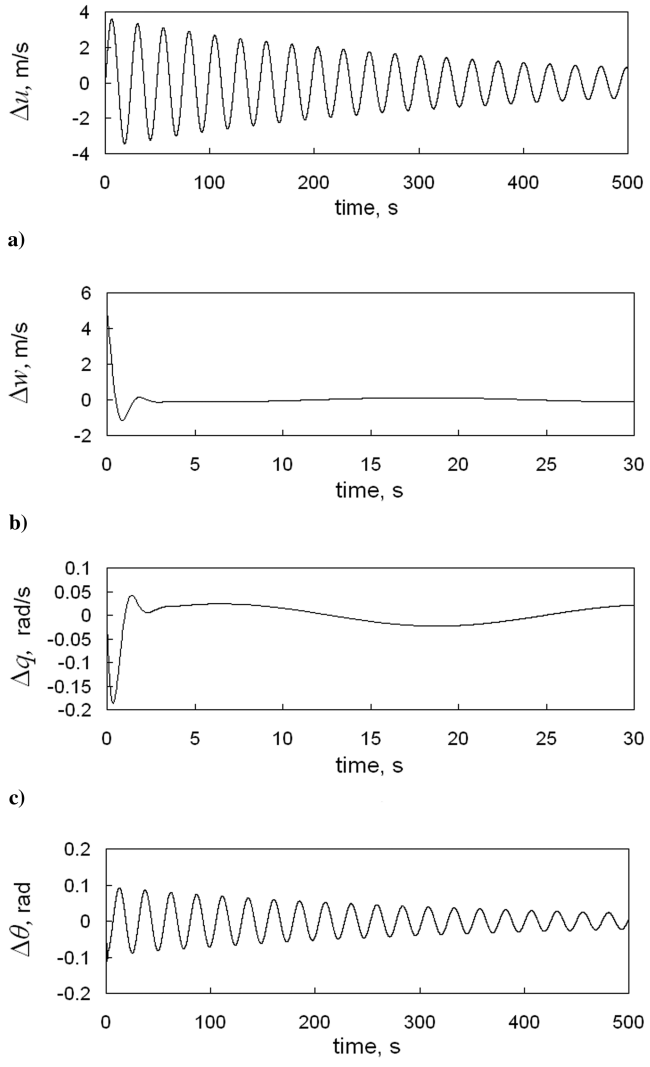

Fig. 2 Longitudinal response of the airplane with variations: a) longitudinal velocity, b) vertical velocity, c) pitch rate, and d) pitch angle.

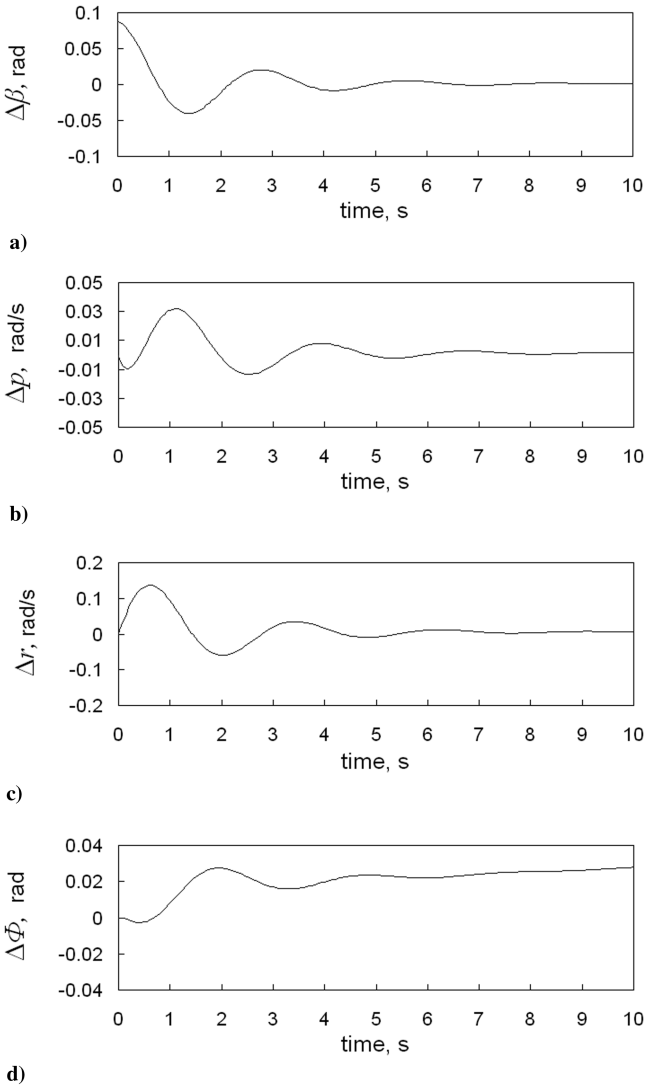

Fig. 3 Longitudinal response of the airplane with variations: a) sideslip, b) roll rate, c) yaw rate, and d) bank angle.

mode equal to 0.01492, greater than 0, based on the requirements given in [25], qualifying for level 2 flying qualities.

An analysis was made to determine the free longitudinal response of the airplane for a given initial disturbance. The corresponding fourth-order differential equations of motion were integrated using the classical fourth-order Runge–Kutta method. Figure 2 shows the response characteristics with initial conditions: $\Delta w = 5$ m/s, $\Delta u = 0.1$ m/s, $\Delta q = 0$, and $\Delta\theta = 0$.

Disturbances in the vertical velocity and pitch rate decay quickly, and they come close to 0 within 3 s. The disturbances in the longitudinal velocity and pitch angle persist for a while and decay slowly. During the short-period mode, disturbances in the vertical velocity and pitch rate decay rapidly. The longitudinal velocity and pitch rate represent the phugoid mode, which continues after the short-period mode has decayed.

Table 3 Lateral-directional dynamic characteristics

	Dutch roll	Roll	Spiral
$t_{1/2}$, s	1.2926	0.1743	14.345
T, s	2.7228	——	——
ζ	0.23132	——	——
ω_n, rad/s	2.3076	——	——

D. Lateral-Directional Motion and Response

The airplane lateral-directional equation of motion consists of the side force, rolling moment, and yawing moment equations of motion [21] formulated in state space $x' = Ax + \eta B$, where $x = [\Delta\beta;\ \Delta p;\ \Delta r;\ \Delta\Phi]^T$ is the state vector and $\eta = [\Delta\delta_a;\ \Delta\delta_r]^T$ is the control vector. The stability matrix A is defined to have the following values for the lateral-directional dynamics of the airplane [21]:

$$A_{\text{lat}} = \begin{bmatrix} -0.1791 & 0.001524 & -1.01307 & 0.23822 \\ -1.43604 & -3.95206 & 1.129161 & 0 \\ 4.4466 & -0.16937 & -0.84687 & 0 \\ 0 & 1 & 0 & 0 \end{bmatrix}$$

The eigenvalues associated with the linearized lateral motion are 1) the Dutch roll mode, $\lambda_{1,2} = -0.5338 \pm 2.245i$; 2) the roll mode, $\lambda_3 = -3.9585$; and 3) the spiral mode, $\lambda_4 = 0.0481$.

A pair of complex roots with damped oscillation with low frequency represent the Dutch roll motion. The Dutch roll mode has a period of 2.7228 s and is well damped, requiring only 1.2926 s to half-amplitude. The root for the roll mode is real and negative, indicating a stable and heavily damped rolling motion; the predicted time to half-amplitude is 0.1743 s. The root for spiral motion is positive, indicating a light divergence spiral motion. It takes 14.34 s to half-amplitude. Table 3 presents the characteristic values for the lateral-directional motion.

The lateral-directional flying qualities of the airplane have been examined using data reported by Prosser and Wiler [25], which lists the requirements for the spiral, roll, and Dutch roll modes.

The maximum roll time constant is 0.0159 s, smaller than the maximum required values for all flying quality levels and flight phases; thus, the airplane is in level 1 during roll mode. The spiral mode already has a time to half-amplitude value of 14.34 s, using the information from [25]; the aircraft studied here has level 2 flying qualities.

The Dutch roll mode has an undamped natural frequency of $\omega_n = 2.30758$ rad/s and a damping ratio of $\zeta = 0.23132$; the product of these two parameters is $(\omega_n \cdot \zeta) = 0.5338$ rad/s. Using [25], the airplane is not expected to encounter any problem at the Dutch roll mode.

The lateral-directional motion of free response of the ANCE was also analyzed. The fourth-order Runge–Kutta method was used to integrate the corresponding fourth-order differential equations. Figure 3 shows the time history of the characteristics for the initial condition: $[\Delta\beta;\ \Delta p;\ \Delta r;\ \Delta\Phi]^T = [0.81\text{ rad};\ 0;\ 0;\ 0]^T$. The disturbance in the sideslip angle induces the rolling and yawing motions. These disturbances decay to 0 within 5–6 s.

IV. Conclusions

A vortex-lattice method was employed to compute the forces and moments acting on the airplane. These were used to compute stability derivatives. The longitudinal and lateral-directional derivates show that the airplane is statically stable.

The open loop longitudinal dynamic stability results show that, for the two modes of longitudinal motion of response, the short-period and phugoid, the reaction is an oscillatory mode describing sinusoidal motion with an amplitude that decreases exponentially with time.

The Dutch roll and roll modes of the airplane match with damped and convergent modes, respectively. However, the spiral mode response prediction corresponds to a divergent mode. This means the airplane is dynamically unstable for the spiral mode, and stable for Dutch roll and roll modes.

The handling qualities for the short-period mode are adequate (level 1) for the mission flight phase, except for the terminal flight phases. For these, the flying qualities are acceptable (level 2). The phugoid mode flying qualities are acceptable (level 2).

The handling qualities for the lateral-directional motion are excellent for the Dutch roll and roll modes for all flight phases (level 1). The flying qualities for the spiral mode are acceptable (level 2).

Acknowledgment

This work was financially supported by the Decanato de Investigación, Universidad Simón Bolívar, Caracas, Venezuela.

References

[1] Boschetti, P., and Cárdenas, E., "Diseño de un Avión No Tripulado de Conservación Ecológica," Engineering Thesis, Dept. of Aeronautical Engineering, Universidad Nacional Experimental Politécnica de la Fuerza Armada, Maracay, Venezuela, 2003.

[2] Cárdenas, E., Boschetti, P., Amerio, A., and Velásquez, C., "Design of an Unmanned Aerial Vehicle for Ecological Conservation," AIAA Paper 2005-7056, Sept. 2005.

[3] Boschetti, P. J., Cárdenas, E. M., and Amerio, A., "Increasing the Lift-Drag Ratio of an Unmanned Aerial Vehicle Using Local Twist," *Journal of Aircraft*, Vol. 45, No. 1, 2008, pp. 10–15. doi:10.2514/1.33353

[4] Melin, T., *User's Guide and Reference Manual for Tornado*, Kungliga Tekniska Högskolan, Stockholm, Sweden, 2000.

[5] Paulson, J. W., "Applications of Vortex-Lattice Theory to Preliminary Aerodynamic Design, Vortex Lattice Utilization," NASA SP-405, 1976, pp. 113–126.

[6] Miranda, L. R., Elliott, R. D., and Baker, W. M., "A Generalized Vortex Lattice Method for Subsonic and Supersonic Flow Applications," NASA CR-2865, Dec. 1977.

[7] Razgonyaev, V., and Mason, W. H., "An Evaluation of Aerodynamic Prediction Methods Applied to the XB-70 for Use in High Speed Aircraft Stability and Control System Design," AIAA Paper 95-0759, Sept. 1995.

[8] Soban, D. S., "Development and Implementation of Software for Rapidly Estimating Aircraft Stability Derivatives and Handling Qualities," NASA CR-201413, Sept. 1996.

[9] Melin, T., "A Vortex Lattice MATLAB Implementation for Linear Aerodynamic Wing Applications," M.S. Thesis, Dept. of Aeronautical and Vehicle Engineering, Kungliga Tekniska Högskolan, Stockholm, 2000.

[10] Bertin, J. J., and Smith, M. L., *Aerodynamics for Engineers*, 3th ed., Prentice–Hall, Upper Saddle River, NJ, 1998, Chaps. 5, 7, 14.

[11] Moran, J., "Wings of Finite Span," *An Introduction to Theoretical and Computational Aerodynamics*, Dover, New York, 2003, pp. 130–135.

[12] Melin, T., "Multidisciplinary Design in Aeronautics, Enhanced by Simulation-Experiment Synergy," Ph.D. Dissertation, Dept. of Aeronautical and Vehicle Engineering, Kungliga Tekniska Högskolan, Stockholm, 2006.

[13] Kier, T. M., "Comparison of Unsteady Aerodynamic Modelling Methodologies with Respect to Flight Loads Analysis," AIAA Paper 2005-6027, Aug. 2005.

[14] Boschetti, P. J., Cárdenas, E. M., and Amerio, A., "Drag Clean-Up Process of Unmanned Airplane for Ecological Conservation," *L'Aerotecnica, Missili e Spazio*, Vol. 85, No. 2, 2006, pp. 53–62.

[15] Williams, J. E., and Vukelich, S. R., "The USAF Stability and Control Digital DATCOM, Vol. 1, Users Manual," McDonnell Douglas Astronautics Company, Rept. AFFDL-TR-79-3032, Saint Louis, MO, 1979.

[16] Cárdenas, E., Boschetti, P., and Amerio, A., "Evaluación de la Estabilidad Estática de un Avión No Tripulado Empleando el Método Vortex Lattice," *Memorias del 9 Congreso Internacional de Métodos Numéricos en Ingeniería y Ciencias Aplicadas*, edited by L. Martino, V. Carrera, G. Larrazábal, and M. Cerrolaza, Sociedad Venezolana de Métodos Numéricos en la Ingeniería y Ciencias Aplicadas, Caracas, Venezuela, 2008, pp. MF37–MF42.

[17] Hoerner, S. F., *Fluid—Dynamic Drag*, published by the author, Bakersfield, California. 1965, Chaps. 6, 8, 13, 14.

[18] Torenbeek, E., "Prediction of the Airplane Polar at Subcritical Speeds in the Route Configuration," *Synthesis of Subsonic Airplane Design*, Deflt Univ. Press, Rotterdam, The Netherlands, 1976, pp. 487–524.

[19] Boschetti, P., "Reducción de Resistencia Aerodinámica en el Avión No Tripulada de Conservación Ecológica," M.S. Thesis, Mechanical and Civil Engineering Depts., Universidad Simón Bolívar, Caracas, Venezuela, 2006.

[20] Brucoli, M. S., "Diseño Estructural de las Alas y Superficies Estabilizadoras del Avión No Tripulado de Conservación Ecológica," B.S. Thesis, School of Mechanical Engineering, Universidad Central de Venezuela, Caracas, Venezuela, 2007.

[21] Nelson, R. C., *Flight Stability and Automatic Control*, 2th ed., McGraw–Hill, Boston, 1998, Chaps. 4, 5.

[22] Cooper, G. E., and Harper, R. P., "The Use of Pilot Rating in the Evaluation of Aircraft Handing Qualities," NASA TN D-5153, 1969.

[23] Hodgkinson, J., *Aircraft Handling Qualities*, AIAA Educational Series, AIAA, Reston, VA, 1998, Chap. 4.

[24] Phillips, W. F., *Mechanics of Flight*, Wiley, Hoboken, NJ, 2004, Chaps. 8, 9, 10.

[25] Prosser, C. F., and Wiler, C. D., "RPV Flying Qualities Design Criteria," U.S. Air Force Flight Dynamics Lab. and Rockwell International Corp., Rept. AFFDL-TR-76-125, Columbus, OH, 1976.